Paramagnetic lead centres in electrolytically coloured KCl:Pb crystals

1995 J. Phys.: Condens. Matter 7 4115

(http://iopscience.iop.org/0953-8984/7/21/011)

J. Phys.: Condens. Matter 7 (1995) 4115–4128. Printed in the UK

Paramagnetic lead centres in electrolytically coloured KCl:Pb crystals

S V Nistor†§, D Schoemaker†, B Briat‡ and V Topa‡§

† Physics Department, University of Antwerp (UIA), B-2610 Wilrijk-Antwerpen, Belgium

‡ Laboratoire d'Optique Physique, ESPCI, 10 rue Vaquelin, 75231 Paris Cedex 05, France

Received 9 February 1995, in final form 5 April 1995

Abstract. Monomer and dimer paramagnetic lead centres have been identified for the first time by electron paramagnetic resonance (EPR) in electrolytically coloured low-purity KCl:Pb crystals. The monomer Pb^-(Rh) centre, with orthorhombic symmetry and local axes [1$\bar{1}$0], [001] and [110], decays completely in darkness and is produced by illumination with visible light. It seems to be related to, but is different from, the so-called Te centres identified in the same samples by their optical and magneto-optical spectra, as well as to the monomer Pb^- centres earlier observed by EPR in high-purity KCl:Pb crystals x-ray irradiated at room temperature. The Tr1 and Tr2 trapped electron lead-dimer centres, with axial symmetry around (111), seem to be related to the Td centres identified by magneto-optical measurements.

1. Introduction

Optical and electron paramagnetic resonance (EPR) studies have shown that in alkali halide crystals containing cation metal impurities from the IB (Cu^+, Ag^+, Au^+) or IVA (Sn^{2+}, Pb^{2+}) groups of elements, it is possible to obtain the corresponding negatively charged metal ions by procedures employed in producing colour centres, i.e. electrolytic or additive colouring, or irradiation with ionizing radiation [1–7].

Several $Sn^-(5p^3)$ and $Pb^-(6p^3)$ negative ions at anion lattice sites, with one or more perturbing entities (primarily anion and cation vacancies) in the immediate vicinity, have been unambiguously identified [6, 7] by EPR spectroscopy in KCl:Sn and KCl:Pb crystals, respectively, after x-ray irradiation at $T > 220$ K. However, EPR spectra attributed to such monomer-type negative ions in samples subjected to additive or electrolytic colouring have not yet been reported.

As shown by optical absorption (OA) studies [2, 8], the electrolytic colouring of KCl:Pb crystals grown from purified salts becomes possible only at temperatures exceeding 500°C. After removing the F centres, by reversing the polarity of the electrodes, the coloured crystals exhibit variations of pink colour. Depending upon various factors, such as the intensity of the applied electric field, the purity of KCl and the concentration of Pb^{2+} ions, several negatively charged species called [2] T centres (Ta, Tb and Tc in [9]) are produced. These centres exhibit somewhat similar optical spectra, consisting [9, 10] of several absorption bands in the UV and visible spectral regions and one simple broad emission band around 6600 cm^{-1}. Based on its diamagnetic properties, as inferred from EPR and magnetic circular dichroism (MCD) measurements [8,11], a structural model consisting of a dimer-type $[Pb^-]_2$ molecular ion at two adjacent anion sites has been suggested for the Ta centre. The OA

§ Permanent address: Institute of Atomic Physics (IFTM), PO Box MG-6 Magurele, Bucuresti - 76900, Romania.

0953-8984/95/204115+14$19.50

spectrum attributed to Tb centres is essentially similar to that of the Ta centres, apart from a blue shift [10]. The temperature dependence of the associated MCD spectra [10] suggests the presence, besides the dominant diamagnetic centre, of at least one paramagnetic centre. The MCD spectra of the Tc centres exhibit [9] clear paramagnetic features.

It has also been reported [9, 12] that new types of negatively charged lead centres with different optical properties are obtained by electrolytic colouring at temperatures as low as 200°C, in high electric fields (5–10 kV cm^{-1}), of KCl:Pb^{2+} crystals grown in air and co-doped with roughly the same amount (10^{17} cm^{-3}) of divalent impurities (Ca^{2+}, Sr^{2+}, Ba^{2+}). The analysis of the resulting MCD spectra has shown [9, 10] that such samples contain new paramagnetic species called Td and Te. The crystals thus obtained exhibit colours ranging from grey to brown, or greenish, with occasionally a touch of purple. The OA and emission spectra attributed [9, 10] to the Td and Te centres are very different from those of the Ta to Tc centres. The OA spectra exhibit less resolved bands and extend down to at least 11 000 cm^{-1} in the near IR. The emission spectra of, for example, Te centres consists of two groups of bands, one at energies higher than 6200 cm^{-1}, the other at lower energies [10]. Moreover, the analysis of the luminescent emissions shows [9, 10] for each Te and Td centre the presence of at least two types of luminescent centres. The same conclusion was inferred from MCD measurements, which have also demonstrated the paramagnetic character of the observed centres [9, 10].

The present paper reports the results of a correlated EPR and MCD study on some of the samples previously investigated by optical techniques [10, 12]. The EPR measurements have resulted in the identification of monomer and dimer paramagnetic lead centres produced by electrolytic colouring in the KCl lattice. It will be shown that the monomer centre, called Pb^-(Rh), is observed only in green–brown samples, being different from the monomer-type Pb^- centres previously observed [7] by EPR in KCl:Pb crystals x-ray irradiated at room temperature (RT). Moreover, it is unstable at room temperature in darkness. It is, however, continuously regenerated from a diamagnetic precursor by daylight illumination at $T > 220$ K. As shown from correlated OA and MCD measurements, the Pb^-(Rh) centre seems to be related to the Te centre, exhibiting optical absorption bands in the 20 000–22 000 cm^{-1} region.

Other EPR spectra with axial symmetry along ⟨111⟩ axes and close values of the spin Hamiltonian parameters, have been observed in the specimens exhibiting optical bands of the Td centres. The analysis of the EPR spectra suggests that the corresponding paramagnetic centres, called Tr1 and Tr2, represent electron-trapped lead dimer centres.

The present study confirms the conclusion of previous magneto-optical studies that various complex diamagnetic and paramagnetic species containing one or more lead ions are produced in KCl:Pb^{2+} crystals by such a low-temperature electrolytic colouring technique. The determination of their structure and production properties is a very complex problem requiring further experimental and theoretical work.

2. Experiment

Several single-crystalline specimens (referred to as S5–S11 and S13) of electrolytically coloured KCl:Pb^{2+} of about 1 cm^3 in size, exhibiting OA and MCD spectra attributed to various T-type centres, have been employed in the present study.

The specimens were cleaved from KCl:Pb^{2+} single crystals grown by the Czochralski method in air, either from purified KCl (specimens S6 and S8), or from pure grade (Reactivul–Bucuresti) KCl containing about 10^{18} cm^{-3} Ca^{2+} ions (specimens S5, S7, S9–S11 and S13). The concentration of the Pb^{2+} ions was roughly 10^{17} cm^{-3} in all samples.

The electrolytic colouring was performed either at about 500°C on crystals grown from KCl, which was initially purified by zone melting, resulting in the pink specimens S6 and S8, or at temperatures in the 265–300°C range and in electric fields of 5–10 kV cm^{-1}, resulting in the brown (S10, S11 and S13), green (S7 and S9), or even colourless (S5) specimens. The low-temperature colouring does not result in the production of F centres, as the amount of electrons injected in the sample is smaller than the amount of Pb^{2+} ions contained in the sample.

OA and MCD spectra were first recorded for each specimen. Afterwards, samples of $3 \times 3 \times 3\text{mm}^3$ were cleaved from each specimen for EPR measurements. The EPR measurements were performed on an ESP 300E BRUKER X-band spectrometer, equipped with a variable-temperature attachment operating in the 10–290 K temperature range, and a microwave cavity which allows *in situ* optical irradiation of the sample in the same temperature range. The optical irradiation at various wavelengths was provided by a 150 W xenon lamp with IR water filter and appropriate sets of cut-off and interference filters.

The experimental set-up for the MCD and OA measurements at pumped helium temperatures was presented in [13]. For all the crystals investigated by MCD the differential absorption $\Delta\alpha$ (cm^{-1}) was measured in a magnetic field of 2.5 T. OA spectra were obtained at 80 K, on a CARY 5E instrument equipped with a cold-finger cryostat also allowing *in situ* illumination. All optical experiments have been conducted on samples handled in daylight.

3. Results

3.1. EPR measurements

EPR spectra attributed to a new type of monomer $Pb^-(6p^3)$ centre were observed at $T \leqslant 35$ K in some of the measured specimens. The spectra (figure 1(*a*)) are characterized by single strongly anisotropic lines, flanked on both sides by weaker doublets. The ratio of the integrated intensities of the singlet to doublet lines is always roughly 3.5 : 1. It means that the EPR spectra originate from defects each involving a single Pb nucleus; the strong single lines are attributed to the even-Pb isotopes (^{204}Pb, ^{206}Pb and ^{208}Pb) with 78% total abundance, which possess nuclear spin $I = 0$, while the doublets originate from the hyperfine (HF) interaction of the unpaired electrons with the ^{207}Pb nuclei (22% natural abundance), with spin $I = 1/2$ and nuclear moment $\mu(^{207}\text{Pb}) = 0.5837\mu_N$. The angular variation of the EPR lines position (figure 1(*b*)) shows that the centre, called Pb^-(Rh), possesses orthorhombic symmetry with the set of axes x, y, z being $[1\bar{1}0]$, [001] and [110], respectively.

The EPR spectra were fitted to the spin Hamiltonian (in the usual notation [14]):

$$\frac{\mathcal{H}}{g_0\mu_B} = \frac{1}{g_0}\boldsymbol{H}\cdot\hat{\boldsymbol{g}}\cdot\boldsymbol{S} + \boldsymbol{S}\cdot\hat{\boldsymbol{A}}\cdot\boldsymbol{I} \tag{1}$$

where $S = 1/2$ and the $\hat{g}$ and $\hat{A}$ tensor axes are along the defect symmetry axes. The second term in (1) occurs if the corresponding nucleus is the ^{207}Pb isotope with nuclear spin $I = 1/2$.

The resulting spin Hamiltonian parameters are presented in table 1, together with the corresponding parameters of the previously reported isoelectronic ($6p^3$) Pb^- and Bi^0 centres [7, 15, 16]. The values of the reduced linewidth $\Delta H = (g/g_0)\Delta H_{exp}$, have also been included. The g and HF tensor principal values of the Pb^-(Rh) centre are similar to

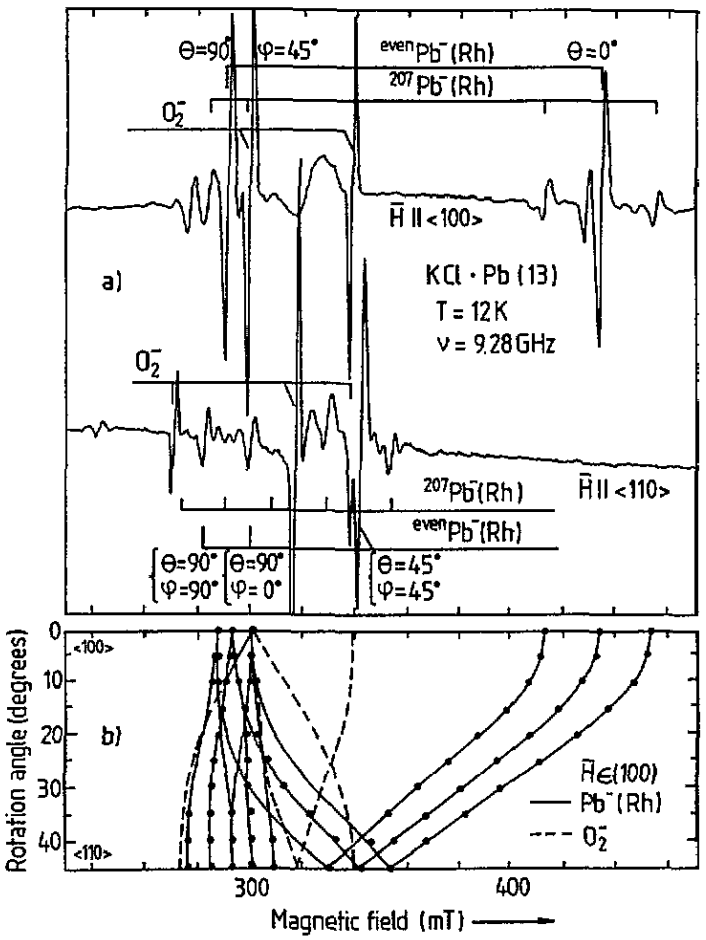

Figure 1. EPR spectra at $T = 12$ K of the monomer Pb^-(Rh) centre in electrolytically coloured KCl:Pb crystals, for the magnetic field $H \parallel \langle 100 \rangle$ and $H \parallel \langle 110 \rangle$. The EPR transitions from $^{even}Pb^-$ and $^{207}Pb^-$ centres making an angle θ with the direction of the magnetic field are marked separately (*a*). The calculated angular variation (full curve) and the experimental line positions (dots) are presented for the magnetic field rotated in a (100) plane (*b*). The line position and angular variation (broken curve) of the O_2^- centres are also presented.

those of the Pb^- centres observed in x-ray irradiated KCl:Pb crystals [7]. This suggests that the Pb^-(Rh) centre is a negatively charged $Pb^-(6p^3)$ ion in an orthorhombic crystal field.

The Pb^-(Rh) centres have been observed in two of the measured specimens (S9 and S13). They are accompanied by EPR lines from the well known [17] O_2^- molecular ion centres, with comparable intensities. The diatomic O_2^- centres exhibit EPR spectra visible below 20 K, described by the first term in (1), with $S = 1/2$ and $g_x = 1.951$, $g_y = 1.955$ and $g_z = 2.436$, and the same orientation of the main axes as the Pb^-(Rh) centre.

Two other EPR spectra, consisting of a stronger central singlet line flanked on both sides by weaker doublets, have also been observed at $T \leqslant 35$ K in some of the investigated specimens. The spectra (figure 2(*a*)), attributed to paramagnetic species called Tr1 and Tr2, exhibit axial symmetry, the symmetry axis being along one of the trigonal ⟨111⟩ axes. The ratio of the integrated intensities of the singlet to doublet lines is roughly 1.8 : 1 for both

Table 1. Experimental EPR parameters of the isoelectronic Pb^- and Bi^0 defects in KCl, and of the resulting crystal-field parameters derived in an intermediate-coupling scheme. The absolute values of the HF parameters A_i from the ^{207}Pb and ^{209}Bi isotope species, respectively, as well as the reduced linewidths $\Delta H = (g/g_0)\Delta H_{exp}$ are given in mT. The accuracy of the presently determined g values and HF parameters A_i are ±0.002 and ±0.2 mT, respectively.

Defect	T (K)	g_x [1$\bar{1}$0]	g_y [001]	g_z [110]	A_x [1$\bar{1}$0]	A_y [001]	A_z [110]	ΔH	$\mathcal{D}/F_2$	$\alpha = \mathcal{E}/\mathcal{D}$	Ref.
Pb^-(Rh)	12	2.337	1.527	2.201	17.4	42	16.2	1.9	−30	−0.006	a
Pb^-(1)	15	3.555	1.151	0.6857	23.8	25.0	18.8	1.7	−26	−0.12	b
Pb^-(2)	15	1.114	3.668	0.6595	4.0	35.6	<5	2.3	−25.7	+0.13	b
Pb^-(4)	15	3.792	1.546	0.9458	<2	18.8	···	2.0	−20	−0.13	b
Bi^0	8	2.7114	1.1078	2.7114	22.11	23.4	22.11	3.1	−22.4	0	c

a This paper. Crystal-field parameters corresponding to a localization factor $f = 0.55$ (see text).
b [7].
c [15, 16]. The centre exhibits axial symmetry around a ⟨100⟩ direction.

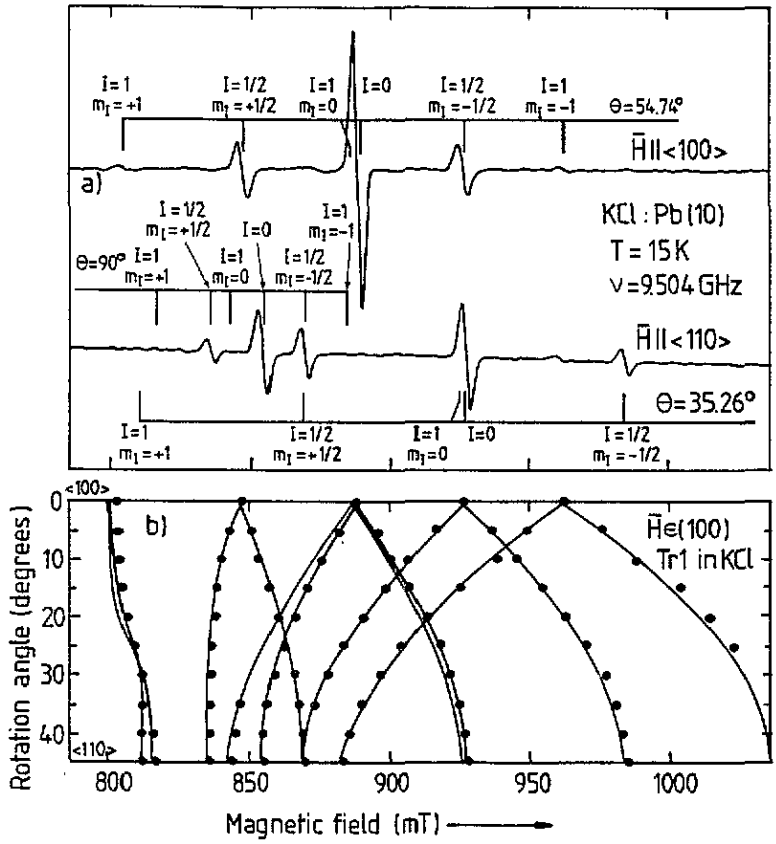

Figure 2. EPR spectra at $T = 15$ K of the dimer Tr1 centre in an electrolytically coloured KCl:Pb^{2+} crystal, for the magnetic field $H \parallel \langle 100 \rangle$ and $H \parallel \langle 110 \rangle$. The various transitions from centres making an angle θ with the direction of the magnetic field are marked by vertical bars (*a*). The calculated angular variation (full curve) and the experimental line positions (dots) are presented for the magnetic field rotated in a (100) plane (*b*).

centres, suggesting in each case a dimer structure involving two lead ions/atoms. Indeed, considering the natural isotope abundance of the lead isotopes one finds that 61% of such dimer centres contain only ^{even}Pb nuclei resulting in the singlet line, 34% contain one ^{207}Pb nucleus and one ^{even}Pb nucleus resulting in the doublet line, and only 5% contain two ^{207}Pb nuclei resulting in a quadruplet (or triplet for magnetically equivalent nuclei) structure. We have been able to observe for the centre Tr1, which has the highest concentration (S10), another pair of weak lines with individual intensity ratios to the singlet line of 1 : 48 and a splitting of roughly twice the splitting of the doublet lines (figure 2(*a*)). As shown from the analysis of the angular dependence of the EPR spectra (figure 2(*b*)), these two lines represent the outer components of the quartet spectrum, the inner two lines being hidden under the strong singlet line.

The EPR spectra of the trigonal centres are described by the spin Hamiltonian

$$\frac{\mathcal{H}}{g_0\mu_B} = \frac{1}{g_0}\boldsymbol{H}\cdot\hat{\boldsymbol{g}}\cdot\boldsymbol{S} + \boldsymbol{S}\cdot\hat{\boldsymbol{A}}\cdot\boldsymbol{I}_1 + \boldsymbol{S}\cdot\hat{\boldsymbol{A}}\cdot\boldsymbol{I}_2 \tag{2}$$

where $S = 1/2$ and $I_1 = I_2 = 1/2$. The $\hat{g}$ and $\hat{A}$ tensors are both axially symmetric about one of the ⟨111⟩ axes. The first term in (2) describes the singlet line spectrum. By including the second and the third terms, one describes the doublet and the quadruplet spectra, respectively. The principal values of the g and A tensors, as determined from the singlet and doublet spectra (table 2), were further employed in the case of the Tr1 centre to predict the positions of the quadruplet spectrum. As shown in figure 2, the position of the outer two transitions ($I_1 + I_2 = I = 1, m_I = \pm 1$) could be identified in a satisfactory manner, considering the low accuracy of the experimental determination due to their small intensity. The calculation also explains the two seemingly absent components $I = 0$, $m_I = 0$ and $I = 1$, $m_I = 0$, which are hidden under the intense singlet line, although the latter one becomes separated for orientations of the magnetic field relative to the local axes around $\Theta = 90°$.

Table 2. Experimental EPR parameters of dimer-type lead centres in alkali halides. The absolute values of the HF parameters A_i and the reduced linewidths $\Delta H = (g/g_0)\Delta H_{exp}$ are given in mT. The accuracy of the presently determined g values and HF parameters A_i are ±0.0005 and ±0.5, respectively.

Defect	T (K)	g_x	g_y	g_z	A_x	A_y	A_z	ΔH	Ref.
Tr1 in KCl	15	0.7950	0.7950	0.6972	35.0	35.0	142.6	1.3	a
Tr2 in KCl	12	0.8438	0.8438	0.6818	39.1	39.1	139.3	1.5	a
Pb_2^{3+}(I) in NaCl	13	1.438	1.222	1.625	122	117	125	5.5	b
Pb_2^{3+}(III) in NaCl	13	1.469	1.300	1.621	123	115	115		b

a This paper. The centre exhibits axial symmetry around a ⟨111⟩ direction.
b [24]. Local axes [1$\bar{1}$0],[001] and [110].

The trigonal Tr1 centre has been observed in several specimens (S5, S7, S10 and S11). The trigonal Tr2 centre could be observed only in one of the specimens (S7), which also contained Tr1 centres. Samples S6 and S8 did not exhibit any EPR spectra that could be attributed to paramagnetic lead centres.

The presence of the O_2^- molecule ions has been detected in specimens S7 and S11, containing different paramagnetic lead centres, suggesting that the O_2^- molecule ions are not directly involved in the structure of these paramagnetic lead centres observed by EPR.

It should also be mentioned that the concentration of paramagnetic lead centres observed by EPR is not constant in different samples cleaved from the same specimen, which means that their distribution is not uniform in the whole volume of the specimen subjected to electrolytic colouring.

3.2. Optical measurements

The pink specimens S6 and S8 exhibit OA and MCD spectra (not shown here), which are correlated to those of the diamagnetic Ta and Tb centres [9, 10]. However, the temperature dependence of the MCD indicates that in both specimens an important amount of additional paramagnetic species is present. Furthermore, although the OA spectra of S6 and S8 are very similar, the MCD spectra show considerable differences. The absence of any EPR transitions in these specimens is consistent with the diamagnetic properties of the Ta and Tb centres as reported earlier [9, 11]. Moreover, it suggests that the additional paramagnetic species revealed by MCD are EPR silent.

Specimens S9 and S13, both containing Pb^-(Rh) centres, with green and brown–green colours respectively, exhibit OA (figure 3(*a*)) and MCD (figure 3(*b*)) spectra correlated [10] to those of the Te type of centres. Actually, even the centre Te and specimen S9, which otherwise have a fairly similar OA spectrum, exhibit striking differences in their MCD spectra, particularly in the 21 000–26 000 cm^{-1} range. As previously noticed [10], all these results indicate that the most salient MCD features are not associated with the dominant OA bands.

A similar conclusion can be drawn from figure 4. Specimen S10 (brown–pink), containing the highest concentration of Tr1 centres, has an OA spectrum (figure 4(*a*)) reasonably well correlated to that of the almost colourless reference specimen S5 (Td), whereas the MCD spectra (figure 4(*b*)) are markedly different, except in the 18 000–21 000 cm^{-1} spectral range.

The OA and MCD spectra of the green coloured specimen S7, containing both Tr1 and Tr2 centres, exhibit broad featureless bands, which have not been further investigated.

3.3. Colour centre production experiments

It has been found that the Pb^-(Rh) centres exhibit specific properties under illumination with visible light. All samples containing such centres exhibit a decrease to half in the concentration of the Pb^-(Rh) centres, after being kept in darkness at RT for about 20 h, and decay completely after about one week of such treatment. However, their initial concentration is restored by keeping the sample at RT, under ambient light, for about 15 min. The bleaching/colouring process is fully reversible and does not affect the EPR lines attributed to O_2^- centres. After one year of experiments we found no change in the maximum attainable concentration of Pb^-(Rh) centres in each investigated sample.

It is obvious that the Pb^-(Rh) centres are unstable at RT, being continuously formed from an EPR silent precursor under illumination with visible light. The production of the Pb^-(Rh) centre from its precursor is not a simple electron (hole) trapping process, but also involves ion (vacancy) movement. Indeed, as shown by *in situ* optical formation experiments under illumination with high-intensity visible light at various temperatures, the Pb^-(Rh) centres are formed only at $T \geqslant 225$ K, i.e. at temperatures where the vacancies of the KCl lattice are mobile [18]. Consequently, it is possible to handle the bleached samples under ambient light, without formation of Pb^-(Rh) centres, just by keeping their temperature below 225 K.

Selective optical formation experiments at RT and various wavelengths, with monochromatic light from the xenon lamp and appropriate sets of cut-off and interference filters, have shown that the Pb^-(Rh) centres are formed in a broad spectral range, extending at least from 14 000–26 000 cm^{-1}.

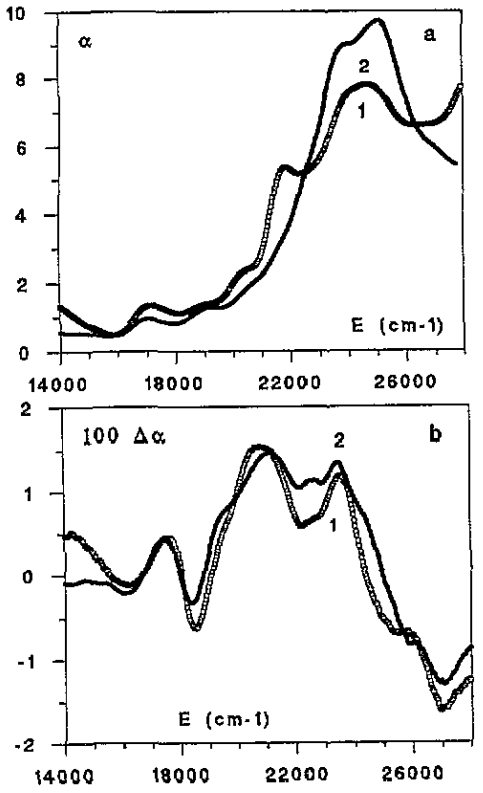

Figure 3. (*a*) OA, $T = 1.4$ K and (*b*) MCD, $T = 4.2$ K of centre Tc (1) and specimen S13 (2). The corresponding spectra of specimen S9 are presented in figure 5.

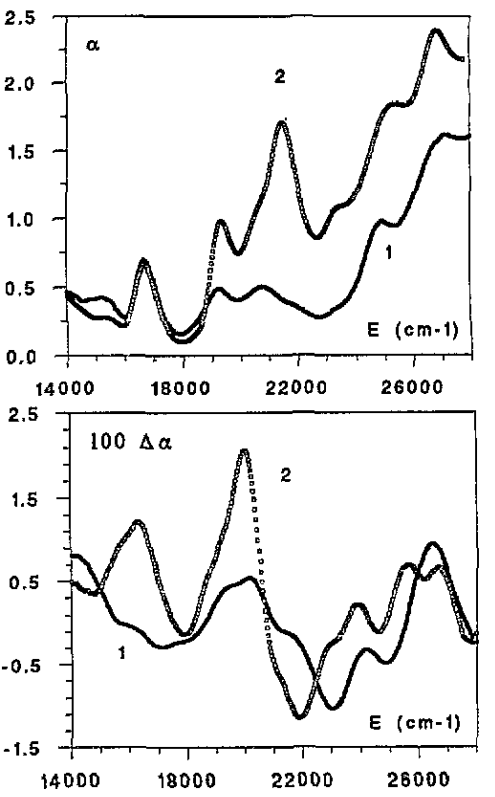

Figure 4. (*a*) OA, $T = 1.4$ K and (*b*) MCD, $T = 4.2$ K spectra of specimens S5 (Td, 1) and S10 (2). For the sake of comparison both α and $\Delta\alpha$ for S10 have been divided by 2.

The possibility of obtaining samples containing controlled amounts of Pb^-(Rh) centres, in principle, offers the possibility of determining their OA and MCD spectra by simply subtracting the spectra of the coloured samples from the spectra of the bleached samples. The procedure is illustrated in figure 5, in the case of specimen S9. Whereas colouration strongly modifies the MCD, the OA suffers only a weak change. The sign of the difference spectra shows that Pb^-(Rh) centres contribute at least in the 20 000–22 000 cm^{-1} spectral region, another paramagnetic centre being destroyed during colouration (MCD at higher energies). These conclusions were reinforced by similar findings in the case of the centre Te and the specimen S13.

Contrary to the Pb^-(Rh) centre, both Tr1 and Tr2 centres are stable at RT, either in darkness or under illumination with visible light.

4. Discussion

The EPR and optical experiments on samples containing Pb^-(Rh) centres show that these centres represent only a small proportion of the total amount of negatively charged lead-associated defects called Te centres, which are responsible for the main optical bands.

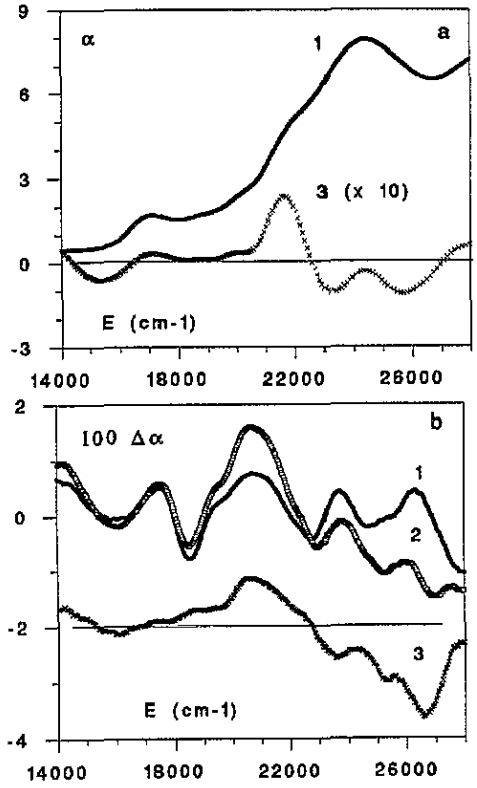

Figure 5. (*a*) OA, $T = 80\,\mathrm{K}$ and (*b*) MCD, $T = 1.4\,\mathrm{K}$ of specimen S9 after one week in darkness (1) and after subsequent illumination of 10 min at RT with unfiltered light (2). Spectrum (3) stands for the difference (2 − 1). Note the magnification factor (×10) in the case of the sole OA spectrum.

However, their occurrence in the same samples suggests that the Pb^-(Rh) and the Te centre are structurally related.

Because it is impossible to change the concentration of the trigonal Tr1 and Tr2 centres, it has not been possible to identify unambiguously their optical bands by production experiments. However, the presence of the trigonal centres only in samples exhibiting a Td type of optical spectra suggests that the Tr1 and Tr2 centres are essentially similar to the Te. At least they represent lead-type defects, i.e. the same basic defect perturbed by different neighbouring vacancies and/or impurities.

In the analysis of the spin Hamiltonian parameters of the monomer Pb^- centres one has to consider the effect of the non-cubic crystal fields due to the neighbouring defects, as well as the likely occurrence of Jahn–Teller (JT) distortions, as in the case of the orthorhombic Pb^- centres produced by x-ray irradiation [7].

Due to the large spin–orbit coupling ($\xi(Pb^-) \simeq 6100\,\mathrm{cm}^{-1}$), the LS coupling scheme is a bad one for the $Pb^-(6p^3)$; it is more appropriate to use an intermediate-coupling scheme between LS and jj. Moreover, the crystal-field strength required to obtain the observed g values is comparable in magnitude to the Coulomb repulsion and the spin–orbit interaction. Consequently, a quantitative description of the ground-state properties requires a full diagonalization of the crystal-field, spin–orbit and Coulomb repulsion terms within the 20 states of the p^3 configuration [7].

Such an analysis shows [7] that in a cubic crystal-field the ground state responsible for the EPR properties is a fourfold-degenerate Γ_8 state. Due to the sizable orbital angular momentum present in this ground Γ_8 quartet, the Pb^- ion in an octahedral anion site is subjected to a mixture of E_g and T_{2g} JT distortions, resulting in local crystal-fields with

orthorhombic symmetry. The large JT energy ($\simeq 2500\,\mathrm{cm}^{-1}$), one order of magnitude larger than the typical phonon energy, results in a static JT distortion. The presence of neighbouring point defects could then be reflected in the stabilization of one of the possible JT distortions, as well as in additional perturbing changes in the local crystal-field. It is thus likely that a large variety of Pb^- defects exists, with large g shifts and various local symmetry axes, as resulting from the combined action of a JT distortion and the presence of neighbouring lattice defects.

The quantitative description of the EPR spectra of Pb^- centres in terms of crystal-field, spin–orbit and Coulomb repulsion in an intermediate-coupling scheme has resulted [7] in a graphical representation (figure 5 of [7]) of the g components as a function of the crystal-field components ratio $\alpha = \mathcal{E}/\mathcal{D}$, where $\mathcal{D}$ and $\mathcal{E}$ are the axial and rhombic components of the crystal-field respectively, and $\mathcal{D}/F_2$ is the ratio of the dominant crystal-field term $\mathcal{D}$ to the Slater–Condon parameter F_2.

In view of the very small deviation from axial symmetry of the Pb^-(Rh) centre, it is possible to perform the analysis of its g components in an axial approximation. In this case, the g components depend only on the $\mathcal{D}/F_2$ ratio. The resulting $g_\parallel$ ($g_\perp$) against $\mathcal{D}/F_2$ curves offer a simple way of determining the $\mathcal{D}/F_2$ ratio of each centre with either $g_\parallel$ or $g_\perp$. In the case of the Pb(Tr) centres a large difference is obtained between the $\mathcal{D}/F_2$ values derived from the $g_\parallel$ (-10) and $g_\perp$ (-37) components, respectively. This large discrepancy should be compared to the case of the orthorhombic Pb^- centres in x-ray irradiated KCl:Pb crystals, where differences of less than 25% were found [7]. The difference between the $\mathcal{D}/F_2$ values resulting from the two g components seem to be only partly due to the neglected small orthorhombicity of the Pb^-(Rh) centre. One also has to remember that the analysis [7] of the energy level splitting of the Pb^- centres was performed in a pure ionic approximation, neglecting any delocalization to the neighbouring ligands.

One can attempt to describe the delocalization effects employed in the rather *ad hoc* manner used to describe the g and hyperfine components of the np^1 centres in alkali halides [18, 19]. A localization factor f was introduced according to the formulae

$$\begin{aligned} g_\parallel &= f g_\parallel^0 + (1-f) g_e \\ g_\perp &= f g_\perp^0 + (1-f) g_e \end{aligned} \tag{3}$$

where $g_\parallel^0$ and $g_\perp$ are the g components in a purely atomic model, described according to [7]. The delocalized part $(1-f)$ of the 6p valence electrons will contribute to the g factor with nearly the free-electron value $g_e = 2.0023$ (the spin–orbit parameters of K^+ and Cl^-, as well as of some possible neighbouring impurities such as Ca^{2+}, Ba^{2+} or OH^-, are small compared to that of Pb^-). Proceeding along this path, formulae (3) and figure 7 yield $f = 0.55$ and, not surprisingly, a more precise value of $\mathcal{D}/F_2 = -30$. According to such an analysis the resulting *atomic* g components of the Pb^-(Rh) centre would be $g_\parallel^0 = 1.07$ and $g_\perp^0 = 2.53$. The corresponding $\mathcal{D}/F_2$ ratio is slightly larger than for the orthorhombic Pb^- centres in x-ray irradiated crystals (table 1). The delocalization factor $(1-f) = 0.45$ would suggest a delocalization of the paramagnetic 6p electrons to the neighbour ligands comparable to that derived for the $Tl^0(1)$ centre, which consists of a $Tl^0(1)$ atom next to an anion vacancy [18].

However, in view of the simplistic way in which covalence has been accounted for, the resulting numerical values have to be regarded as semiquantitative. The presence of a neighbouring negative anion vacancy next to the Pb^- ion, as suggested by the above analysis, is not surprising considering the presence in the crystal lattice of a large number of anion vacancies induced by the electrolytic colouring process.

Any structural model of the Pb^-(Rh) centre should be consistent with the observed local orthorhombic symmetry, should consider possible neighbouring vacancies and/or impurities (such as Ca^{2+}), and explain its reversible formation/bleaching above 220 K, which suggests a site-switching process.

Several structural models of the Pb^- (Rh) centre consisting of a substitutional or interstitial Pb^- ion in the KCl lattice with various neighbouring vacancies/impurities can be imagined. Moreover, structural models in which the Pb^- ions are embedded in aggregates or even in a precipitated Suzuki phase cannot be excluded, if one considers that the electrolytic colouring has been performed in the temperature range where precipitation of Ca^{2+} ions [20] and/or Pb^{2+} ions [21, 22] takes place. However, the available data do not allow us to determine its exact structure. Additional experimental data, especially ENDOR measurements, may give the required information concerning the nature and position of the neighbouring ligands.

As shown from the analysis of the EPR spectra, the trigonal Tr1 and Tr2 centres consist of dimer Pb_2-type centres. The mutually similar g and HF parameters strongly suggest that the two centres originate from the same Pb_2-type dimer, but with slightly different surroundings. The small HF splittings, compared to those of the trapped-hole lead centres (see table 23 of [23]) suggests that we are observing trapped electron configurations. Trapped-electron lead dimer centres, in which one or more electrons are trapped at pairs of neighbouring Pb^{2+} ions, have to be considered.

The simplest one is the Pb_2^{3+} centre, observed [24] in x-ray irradiated NaCl:Pb crystals. The corresponding spin Hamiltonian parameters of two of those centres are presented in table 2. Their electron configuration, which is complementary to that of the self-trapped hole V_k centre [25], consists of a single valence electron trapped at two $Pb^{2+}(6s^2)$ ions in a molecular σ_g orbital which is considered as a linear combination of atomic orbitals, namely

$$\sigma_g = \alpha_g(6s_1 + 6s_2) + \beta_g(6p_{z,1} - 6p_{z,2}). \tag{4}$$

The excited $\pi_g^x = \mu_g(6p_{x,1} - 6p_{x,2})$ and $\pi_g^y = \mu_g(6p_{y,1} - 6p_{y,2})$ orbitals are mixed into σ_g by the spin–orbit interaction, and separated from the ground state (orthorhombic symmetry) by excitation energies E_{1g} and E_{2g}, respectively. The excitation energies can be determined from the $\Delta g = g_e - g_i$ shifts by a perturbation calculation to the second order, with the spin–orbit coupling as a perturbation [25]. The complete expressions for a Pb_2^{3+} centre in an orthorhombic crystal field are given in [24].

A calculation performed with the same approximations as in [24] results in values of $E_g = 1.066$ eV and $\delta = 0.031$ for the Tr1 centre and $E_g = 1.068$ eV and $\delta = 0.016$ for the Tr2 centre, where $E_g = E_{1g} = E_{2g}$ for the axial symmetry. The resulting excitation energies E_g are comparable, although smaller than those found in the case of the isoelectronic Pb_2^{3+}(III) centre [24] in NaCl ($E_{1g} = 1.07$ eV and $E_{2g} = 2.75$ eV), or of the axial $Tl_2^+\langle 111\rangle$ centre [26] in KCl ($E_g = 1.80$ eV). However, the resulting values of the parameter δ, which is the matrix element of the orbital angular momentum between σ_g and π_g, are unreasonably small and difficult to understand if one compares them with the corresponding values of $\delta = 0.3$ for the Pb_2^{3+}(III) centre in KCl and $\delta = 0.56$ for the $Tl_2^+\langle 111\rangle$ centre in KCl. Even the values for the latter two centres are considered to be quite small.

Another possible trapped-electron lead dimer centre is the Pb_2^+ centre, resulting from the consecutive trapping of three electrons at a pair of neighbouring Pb^{2+} ions. The electron configuration of this dimer centre, which can be considered to originate from a negatively charged Pb^- ion next to a Pb^{2+} ion, consists of a filled σ_g molecular orbital with the unpaired electron in the π_g^x molecular orbital. Due to the π character of the unpaired

electron, a very small isotropic HF component is to be expected in comparison with the Pb_2^{3+} centre. However, as can be easily seen from the values presented in table 2, the isotropic HF components of the HF tensors for both Tr1 and Tr2 centres are comparable with those of the Pb_2^{3+} centre. Paramagnetic molecular lead ions with a larger number of trapped electrons, such as Pb_2^- or Pb_2^{3-}, with the unpaired electron in a π_g^y or π_u^x molecular orbital, also seem to be unlikely, for the same reasons as the Pb_2^+ centre.

A close examination of the spin Hamiltonian parameters of the trigonal lead dimer centres Tr1 and Tr2 (table 2) shows that both centres exhibit g values close to 2/3, which, according to the Landés formula, is the g value of the ground state of a free atom in a $6P_{1/2}$ state. Such an electron configuration corresponds to a Pb^+ ion in a weak crystal field [18]. The above observation suggests a possible structure for the core of the Tr1 and Tr2 centres consisting of a pair of weakly interacting Pb^{2+} ions along a ⟨111⟩ direction which have trapped an electron. For reasons which are yet unclear, the paramagnetic electron is mainly localized at one of the Pb^{2+} ions. The tunneling of the paramagnetic electron to the other Pb^{2+} ion would result in g values close to those of the Pb^+ centres [18] and HF splittings at most half as large. A possible structural model consists of a pair of Pb^{2+} ions at substitutional neighbouring cation sites in the KCl lattice, along a ⟨111⟩ direction. The presence of two slightly different centres (Tr1 and Tr2) could then be further explained by the presence in one of the centres of a weakly perturbing neighbouring defect, such as a Ca^{2+} ion.

As in the case of the Pb^-(Rh) centres, the formation of the trigonal dimer-type lead centres in a precipitated phase of impurity ions (Ca^{2+} and/or Pb^{2+}) cannot be excluded.

5. Summary and conclusions

Earlier luminescence and MCD measurements [9, 12] on low-purity KCl:Pb crystals containing negatively charged lead centres produced by electrolytic colouring at low temperatures and high electric fields have demonstrated that several types of such centres with different structural and electronic properties are produced in each sample. The present study confirms this conclusion, reporting the identification in low-purity KCl:Pb crystals grown in air of new monomer- and dimer-type lead centres. They seem to be related to, but different from, the negatively charged lead centres observed by optical and MCD spectroscopy in the same crystal, as well as from the other four types of monomer Pb^- centres observed [7] in x-ray irradiated high-purity KCl:Pb crystals grown in a reactive atmosphere.

The Pb^-(Rh) centre with tetragonal symmetry around an ⟨001⟩ axis and a slight rhombic distortion along a set of perpendicular axes, for example ⟨1$\bar{1}$0⟩ and ⟨110⟩, has been observed in specimens containing optical spectra attributed to the Te type of negatively charged lead centres. It has been found that the Pb^-(Rh) centres decay at RT, in darkness, but can be reversibly formed by bleaching at RT with light in the visible range. The absence of any important change in the optical absorption of samples containing either Pb^-(Rh) centres or their precursor, indicates that they represent a very small amount of the negatively charged lead centres observed by optical spectroscopy, to which they seem, however, to be related. MCD measurements suggest that they absorb light in the 20 000–22 000 cm^{-1} region.

The quantitative interpretation of the EPR parameters of the Pb^-(Rh) centre is based on a coupling scheme intermediate between LS and jj, previously developed [7] for the orthorhombic Pb^- centres observed in x-ray irradiated high-purity KCl:Pb crystals. The analysis also suggests a sizable delocalization of the 6p electrons to the neighbouring

ligands, possibly due to the presence of a neighbouring anion vacancy. Criticism may be leveled against the *ad hoc* manner of introducing the delocalization of the 6p electrons. Nevertheless, this pragmatic approach, already successfully employed in understanding the structural and EPR properties of $Tl^0(6p^1)$ centres in alkali halides, offers a possibility to better understand the properties of the Pb^-(Rh) centre in the KCl lattice host.

In the orthorhombic Pb^- centres, previously observed [7] in high-purity KCl:Pb^{2+} crystals after x-ray irradiation, the Pb^- ions are subjected to slightly different orthorhombic crystal-fields, which could be described in the intermediate scheme without significant delocalization. It now seems obvious that in such centres the main source of the local crystal-field is the JT distortion, which is slightly perturbed by lattice defects further away from the Pb^- ion. The structure of the Pb^-(Rh) centre produced in low-purity KCl:Pb^{2+} crystals is strongly influenced by the presence of neighbouring anion vacancies, which are produced in large amounts by electrolytic colouring, resulting in a strong delocalization of the $6p^3$ electrons.

Two types of paramagnetic centres, with trigonal symmetry around a ⟨111⟩ axis and close spin Hamiltonian parameters, called Tr1 and Tr2, identified as electron-trapped dimer-type lead centres, have been observed in samples containing Td-type centres, as identified by their optical spectra. MCD measurements suggest they absorb light in the 18 000–21 000 cm^{-1} region. Neither the Pb_2^{3+} nor the Pb_2^+ molecular centres, resulting from the trapping of one or three electrons at a pair of neighbouring Pb^{2+} ions, respectively, seem to explain the observed spin Hamiltonian parameters.

It is suggested, as a possible core of the trigonal centres, a pair of weakly interacting Pb^{2+} ions at substitutional cation sites of the KCl lattice, along a ⟨111⟩ axis, which have trapped an electron. The observed g values, close to the $g_J = 2/3$ value of a free $Pb^+(6P_{1/2})$ ion, are explained as resulting from a strong localization of the paramagnetic electron at one of the two Pb^{2+} ions. The dimer character of the observed centres would result from the tunneling of the paramagnetic electron between the two equivalent Pb^{2+} ions, a process which could be favoured by other neighbouring defects.

It has also been pointed out that the task of establishing structural models for the observed defects is complicated by the possible presence of Suzuki phases of the Pb^{2+} and/or Ca^{2+} impurity ions, which could be formed during the electrolytical colouring of the sample around 200 K.

It is also not yet clear whether the oxygen-related molecular anion impurities play any role in the formation and structure of the newly discovered trapped-electron lead defects.

The results of this study clearly show that the low-temperature electrolytical colouring of KCl:Pb crystals co-doped with alkali earth impurities produce new types of point defects. However, any further substantial progress in elucidating the nature and properties of the observed electron-trapped lead centres requires their controlled production, as well as further spectroscopical investigations and extensive theoretical analysis of the spin Hamiltonian parameters for various electron configurations of monomer and dimer electron-trapped lead centres, in which relativistic effects, important for such a heavy ion, should be included

Acknowledgments

The authors would like to thank E Goovaerts for helpful discussions. One of the authors (SVN) is grateful to the University of Antwerpen (UIA) for a research scholarship during the time this research project was performed. Another author (VT) is grateful to the Commission of the European Communities for the award of a grant. The OA and MCD work was supported by the French CNRS.

References

[1] Topa V 1967 *Rev. Roum. Phys.* **12** 781
[2] Topa V and Velicescu B 1969 *Phys. Status Solidi* b **33** K29
[3] Fisher F 1970 *Z. Phys.* **231** 393
[4] Kleeman W 1968 *Z. Phys.* **214** 285; 1971 *Z. Phys.* **24** 145
[5] Tsuboi T 1977 *Can. J. Phys.* **55** 1316; 1978 *Physica* **95B** 397; 1979 *Physica* **96B** 341
[6] Van Steen F and Schoemaker D 1979 *Phys. Rev.* B **19** 55
[7] Goovaerts E, Nistor S V and Schoemaker D 1982 *Phys. Rev.* B **25** 83
[8] Velicescu B and Topa V 1973 *Phys. Status Solidi* b **55** 793
[9] Topa V, Briat B and Apostol E 1993 *Proc. 12th Int. Conf. on Defects in Insulating Crystals, Nordkirchen 1992* ed O Kanert and J-M Spaeth (Singapore: World Scientific) p 565
[10] Topa V, Briat B, Rivoal J C, Pedrini C and Moine B 1994 *J. Lumin.* **60–1** 603
[11] Billardon M, Briat B, Topa V and Taurel L 1970 *Proc. 16th Congress AMPERE* ed I Ursu (Bucharest: RSR Academy) p 423
[12] Topa V, Iliescu B and Apostol E 1993 *Proc. 12th Int. Conf. on Defects in Insulating Crystals, Nordkirchen 1992* ed O Kanert and J-M Spaeth (Singapore: World Scientific) p 462
[13] Moya E, Zaldo C, Briat B, Topa V and Lopez F J 1993 *J. Phys. Chem. Solidi* **54** 809
[14] Abragam A and Bleaney B 1970 *Electron Paramagnetic Resonance of Transition Ions* (Oxford: Oxford University Press)
[15] Nistor S V 1988 *Solid State Commun.* **66** 995
[16] Goovaerts E, Nistor S V and Schoemaker D 1990 *Phys. Rev.* B **42** 3810
[17] Känzig W and Cohen M H 1959 *Phys. Rev. Lett.* **3** 509
[18] Goovaerts E, Andriessen J, Nistor S V and Schoemaker D 1981 *Phys. Rev.* B **24** 29
[19] Ahlers F J and Spaeth J-M 1986 *J. Phys. C: Solid State Phys.* **19** 4693
[20] Andreev G A and Klimov A V 1978 *Phys. Status Solidi* a **46** 421
[21] Garcia-Sole J, Zaldo C and Aggulo-Lopez F 1979 *Rad. Eff.* **73** 131
[22] Nistor S V and Stoicescu G D 1990 *St. Cerc. Fiz.* **42** 381
[23] Nistor S V, Schoemaker D and Ursu I 1994 *Phys. Status Solidi* b **185** 9
[24] Heynderickx I, Goovaerts E and Schoemaker D 1987 *Phys. Rev.* B **36** 1843
[25] Schoemaker D 1973 *Phys. Rev.* B **7** 786
[26] Nistor S V, Goovaerts E, Yang B R and Schoemaker D 1983 *Phys. Rev.* B **28** 1219